THE DESIGN OF POST-BUCKLED SPINAL STRUCTURES FOR AIRFOIL SHAPE CONTROL USING OPTIMIZATION METHODS

Narcis M. Ursache, Neil W. Bressloff and Andy J. Keane
Computational Engineering and Design Group,
University of Southampton, Highfield, Southampton, SO17 1BJ, UK.

E-mail: narcisu@soton.ac.uk, nwb@soton.ac.uk, ajk@soton.ac.uk

ABSTRACT

In this paper we examine the use of optimization methods and a variety of shape definition schemes to design spinal structures for the control of deformable shape airfoils. The aim is to find structures that, when suitably loaded, can be used to alter the aerodynamic performance of a cladding that forms the airfoil. Further, by using structures that are acting in the post buckling regime it is possible to obtain significant changes in shape with only modest changes in applied load.

INTRODUCTION

Flapless, variable geometry airfoils are not a new idea: the original Wright Brothers Flyer used "wing warping" to provide flight control. There is, however, a great deal of current interest among aircraft designers in shape control systems that work without conventional slats and flaps, with their associated discontinuities, hinge lines and gaps. Primarily this is because engineers seek designs that have low radar signatures or are very quiet in operation. When controlling the shape of a wing for such roles only internal mechanisms can be used and a flexible outer cladding forms the aerodynamic surface. Given the space and weight restrictions that apply inside aircraft wings, design requirements lead to the need for simple yet powerful ways of controlling the airfoil external shape. Such devices must also be extremely reliable and have low maintenance and operational power requirements.

The structural system considered here would be coupled by a flexible foam core to a conformable aerofoil surface to achieve the desired control effects. The main thrust of this paper is to demonstrate the use of optimization based inverse design methodologies to configure a deformable internal spinal structure that could produce shape control with a very limited number of low-power actuators. By using non-linear structural effects this addresses some of the key problems identified in existing work in this field, i.e., the complexity of the internal actuator schemes currently needed, the difficulties associated with scaling them to relatively large, heavily loaded airfoils and excessive power consumption[1]. In this last reference the authors recommend the need to optimize the actuator distribution and the wing configuration – something that is intrinsic to the current work, and with a reduced number of actuators made possible by the non-linear structural response being exploited. This is achieved by adopting a pre-loaded internal spinal system that moves through the desired shape changes under the control of a very limited number of actuators (in an aircraft just one each for the two tip cambers, one for each wing twist and one for the common root camber). In effect control system complexity is traded for passive structural sophistication. This provides a low-power, light weight means of aerofoil shape control with independent control of camber and twist[2].

SHAPE CONTROL CONCEPT

Perhaps the simplest way to envisage the spinal structural approach proposed is to consider a partially buckled simply supported Euler strut subject to an eccentric end load, as depicted in figure 1. As is well known such a strut takes up a half sine wave shape whose amplitude is controlled by the end loading. Moreover, this amplitude is linked to the end-loading in a highly non-linear way, so that modest increases in load result in significant changes in shape (see figure 2).

Next let the properties of the strut vary along its length. In such cases the shape adopted ceases to be a pure sine wave and becomes dependent on the way the strut properties vary. With an appropriate choice of properties the buckled shape can be made to conform to the camber line of an airfoil. Now as the end load is varied we have a means of varying the camber line. If the strut is then connected to a semi rigid pre-tensioned elastic skin via a flexible foam core this affords a means of aerofoil section shape control. The selection of properties is here accomplished via an inverse design procedure

whereby an optimizer is used to control the structural properties and end loads and a commercial FEA code (Abaqus) is used to asses the deformed shape. The objective function used is the sum of the square of the differences between the desired and actual deformed shapes.

Figure 1: Example of a beam-column with eccentric load.

By extruding the strut into a plate and linking this to a wing surface with actuators acting along its edge, full wing shape control becomes possible. Moreover, the principal set of shapes the wing can take up is not set by the actuators and controllers; rather it is determined *a priori* by the structural system – this provides a very efficient and low-powered way of achieving overall shape control. It is also simple and thus reliable. This novel approach is in contrast to the systems researched in the literature where complex actuator setups and sophisticated controllers are used to achieve the desired shapes, which are perhaps better targeted at localised control of shape. A key feature of the proposed spinal structure approach is that the passive structural elements act to distribute simple actuator effects smoothly into the external surface of the wings, thus avoiding undesirable localised features in the surface such as ripples or bulges[3].

STRUCTURAL MODEL

These days the analysis of all but the simplest structures is carried out with the aid of computer programmes, and in particular via finite element analysis (FEA). FEA provides a way of solving complex non-linear equations and implementing theoretical and mathematical methods of physical behavior. Since the loads of interest here are greater than the Euler buckling load, the large deflections encountered are tackled by iterative techniques. Solutions to such nonlinear problems can be found with various different methods: the most commonly used are the single-step and iterative (multi-step) procedures (Euler method, Second order Runge Kutta)[4] and incremental-iterative methods (Newton-Raphson)[5, 6, 7, 8].

In order to understand a model which can be developed to study spinal structures, we begin by considering a pin-ended column subjected to an axial eccentric load (see again figure 1). Here the control force is applied outside the axis of the column so a concentrated moment equal to the force multiplied by the eccentricity appears in every section of the column. Therefore any structural model used must allow for bending and buckling of the column.

In simple linear analysis, the deflection of a perfect beam is indeterminate at the critical axial load, because of the nature of the differential equations used for calculating the deflections. The equation governing bending of beams according to the Euler-Bernoulli beam theory is

$$\frac{d^2}{dx^2}\left(EI\frac{d^2w}{dx^2}\right) - f = 0 \qquad (1)$$

where w is the transverse deflection, E is the modulus of elasticity, I is section inertia and f is transverse loading.

Beyond the critical (Euler) axial load there will be no indefiniteness in the value of the deflection and very large deflections occur for modest increases in load. The shape of the resulting elastic curve is called the *elastica*. The small displacement hypothesis, usually accepted for stress analysis of structures is, of course, not suitable in such circumstances. The elementary theory neglects the square of the first derivative in the curvature formula and provides no correction for the shortening of the moment arm as the loaded end of the beam deflects. The equations governing the large-deflection bending of elastic beams are:

$$-\frac{d}{dx}\left\{EA\left[\frac{du}{dx}+\frac{1}{2}\left(\frac{dw}{dx}\right)^2\right]\right\} - q = 0 \qquad (2.1)$$

and

$$\frac{d^2}{dx^2}\left(EI\frac{d^2w}{dx^2}\right) - \frac{d}{dx}\left\{EA\frac{dw}{dx}\left[\frac{du}{dx}+\frac{1}{2}\left(\frac{dw}{dx}\right)^2\right]\right\} - f = 0 \qquad (2.2)$$

where u is the longitudinal displacement, A is the cross-sectional area and q is the axial distributed load. This set of non-linear equations reverts to equation (1) if the slope $dw/dx \approx 0$, and then the terms $du/dx \approx 0$ and $(du/dx)^2 \approx 0$ [9].

We have plotted the force vs maximum lateral displacement in the y-direction for columns with different eccentricities (assuming the length of the deflected centroidal axis of the column remains the same) using the commercial FEA tool Abaqus 6.3.1, figure 2.

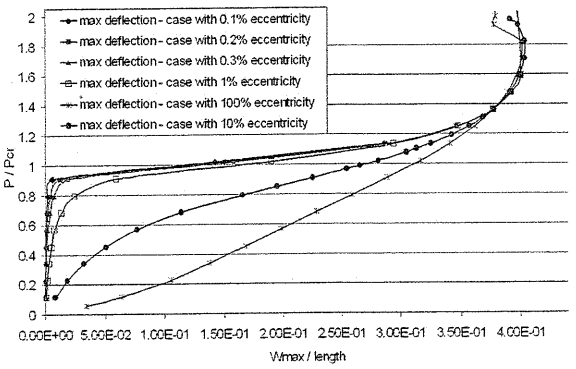

Figure 2: Behavior of beam-columns in non-linear regime, with different eccentricities.

The beam elements in Abaqus use linear, quadratic (allowing transverse shear strain, where the cross section may not necessarily remain normal to the beam axis - Timoshenko beams) and cubic interpolation (in the context of large rotations and small strains, using the Euler-Bernoulli assumptions). For large deflection solutions, the kinematic relationships are not linearized and the problem is solved iteratively, whereby the results of the last run are used as starting values for the next, until convergence conditions are fulfilled, typically a balance of forces. Abaqus breaks the simulation into a number of time increments. At the end of each increment, it finds an approximate equilibrium configuration. For each increment, it takes several iterations using the Newton method, to find an acceptable solution [7].

The curves in figure 2 show the non-linear behavior of the beam-column, as a fraction of the Euler critical load. The greater the eccentricity is, the greater the concentrated moment at the end of beam-column. Consequently, the buckling behavior is not as dramatic as for a classical column. Moreover, increasing the load after the critical state is reached causes the lateral deflection to continue to increase as the load rises, but the stiffness remains positive ($P/Pcr \geq 1$), which indicates the beam-column has a post-critical reserve strength.

The aim here for our spinal structure is to gain control of large displacements using small force variations. The more the eccentricity is increased the greater the slope of the force displacement curves [6, 9]. Therefore, a small eccentric loading gives us the desired effect. Given all these data, we choose to analyze beams with 0.3% eccentricity as this assures robust solution convergence in Abaqus, while still giving significant deflections for small force changes. We have found that with only 0.1% eccentricity numerical instabilities can occur during optimization, due to the widely varying stiffness of the discretized elements needed.

OPTIMIZATION

1. Search Process

To establish the design parameters we seek and to generate equivalent *.inp* files for submitting into Abaqus we have used the *Options* optimization tool[10]. The purpose of this is to simultaneously modify the design and fix the end loading in such a way as to minimize an objective function which, in some sense, characterizes the aerodynamic suitability of the structure:

$$f = \min \sum_i (w_{desired,i} - w_{deflected,i})^2 . \qquad (3)$$

This objective function is the difference between the desired deflected shape – here given by second degree equations based on NACA four digit airfoils[11] and the deflected shape obtained from the lateral deflected nodal positions in the Abaqus solution.

Two codes have been developed to interface with the Options programme. The first code creates the *.inp* file to be submitted to the Abaqus Solver, which is regenerated at every step taken during the optimization. The second code returns the data produced by Abaqus and creates the objective function. These two codes have been linked together within Options (see figure 3). We have then used two stochastic search engines to find the required shapes and end loads: a Genetic Algorithm (GA) and Simulated Annealing (SA), both already implemented in Options. Both methods have the ability to avoid becoming trapped in local minima.

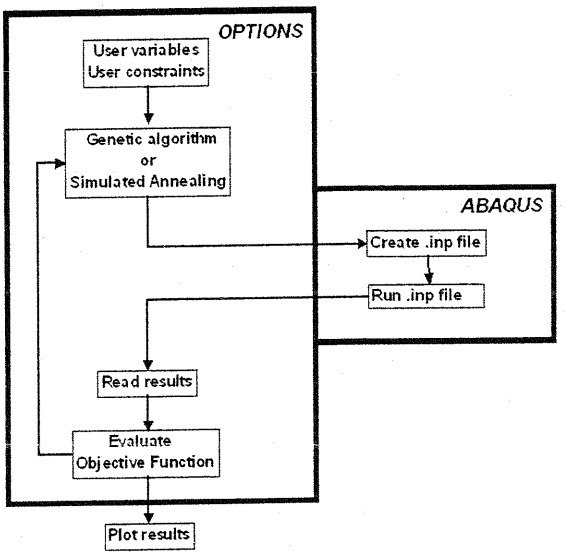

Figure 3: Design System Structure

A Genetic Algorithm imitates the natural evolution process by stochastic means, achieving an optimum solution via an artificial selection method, applied over a number of generations. Its applicability is very good even in complex optimization problems, because it doesn't require complementary attributes for the objective function such as continuity or differentiability. GAs search from one population of solutions to another, rather than from individual to individual. Here, a GA with a population of 100 members is used over 50 generations.

Simulated Annealing is a Monte Carlo approach for minimizing multivariate functions. SA exploits an analogy between the way in which a metal cools and freezes into a minimum energy crystalline structure (the annealing process) and the search for a minimum in a more general system. To apply simulated annealing, the system is initialized with a particular configuration, generated by imposing a random displacement. The algorithm is based on a Metropolis step[12], which was proposed first as a means of finding the equilibrium configuration of a collection of atoms at a given temperature. The algorithm employs a

random search which not only accepts changes that decrease objective function f, but also some changes that increase it. The latter are accepted with a probability

$$p = \exp\left(-\frac{\delta f}{T}\right) \tag{4}$$

where δf is the increase in f and T is a control parameter (i.e., "temperature" in the original application).

2. Parameterization Techniques

The aim of parameterization techniques is to build functions that describe curves and surfaces which are flexible enough to represent a wide range of desired shapes. They should be easily controlled, increasing in this way the number of potential solutions that may be considered. Moreover, if one global parameterization gives a design satisfactorily close to a desired shape, we may begin seeking an improved design using as the starting point the last best solution, by parameterizing the shape perturbations[13,14]. Therefore, a solution can be an algebraic sum of different parameterizing functions. Shape parameterization is the first step in Multidisciplinary Shape Optimization. A number of different techniques are described in Samareh's papers[11,15,16].

➢ Discrete Approach

Initially we have adopted a Discrete Approach technique, using a subset of the finite element grid-point coordinates as design variables. To begin, we have parameterized 14 sections along the beam as in figure 4 (more sections would be computationally more expensive to search), which shows the section variations along the beam following the optimization process.

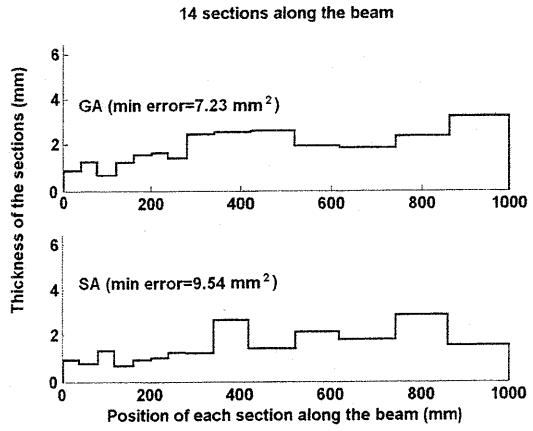

Figure 4: Discrete approach thickness distributions for optimized models to yield 1% NACA camber line when buckled.

To achieve a given deflected shape (e.g., 1% NACA camber line with the position of maximum camber at 25% length) we varied the cross-sectional area by parameterizing the thickness distribution along the beam while the width of the discretized elements remained fixed (here 8 mm – the case with both thickness and width variable is again more computationally expensive to search). The results of searching using this approach while also allowing the optimizer to control the end load are depicted in figure 5, which shows how close the optimized shape of the beam is to the desired camber. Using this approach it is, however, difficult to maintain smoothness of the geometry and the resulting shapes are somewhat impractical to manufacture.

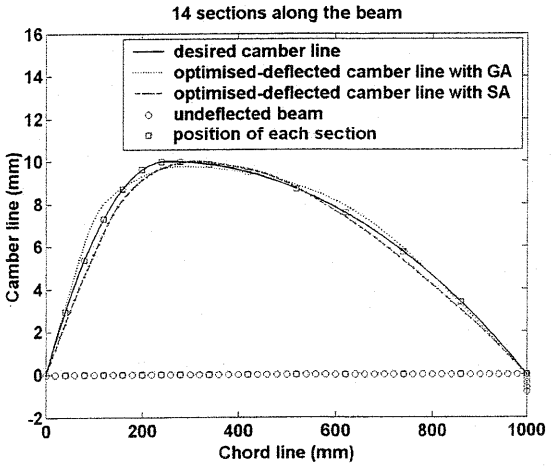

Figure 5: Optimized camber lines obtained with the Discrete Approach technique for 1% NACA camber line, using GA (min. error=7.23 mm^2) and SA (min. error=9.54 mm^2).

➢ Alternative Parameterizations

An alternative parameterization is given by *Hicks-Henne* curves, which provide a compact formulation commonly used in airfoil section parameterization [17, 18]. Using these curves, we have again chosen to generate a thickness distribution along the beam, while the width of each section is constant. Here, the thickness variation is given by

$$b(x) = A\left[\sin\left(\pi x^{\frac{\ln 2}{\ln x_p}}\right)\right]^t, \quad x \in [0,1] \tag{5}$$

where $b(x)$ is the height of the bump, x_p is the location of the peak of the bump and t is a parameter that controls the width of the bump. The resulting distribution is depicted in figure 6 while figure 7 shows the deflected shapes of the optimized cambers using GA and SA searches, again compared to the desired camber line.

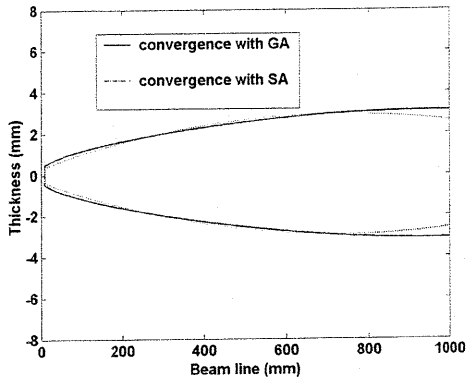

Figure 6: Optimal thickness distributions with Hicks-Henne parameterization.

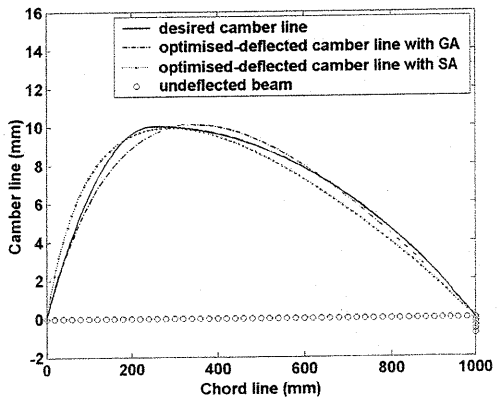

Figure 7: Optimized camber lines obtained with the Hicks-Henne parameterization using GA (min error=11.07 mm^2) and SA (min error=31.97 mm^2).

A *polynomial* approach has also been used to assign the thickness distribution to the beam-column:

$$\overline{R}(u) = \sum_{i=0}^{n-1} \overline{c}_i \overline{u}^i \qquad (6)$$

where n is the number of design variables, and u is the parameter coordinate along the curve. Since the family of polynomial equations is quite large, we have optimized the beam by using a quartic-spline representation as used in the camber definition of the NACA four digit airfoils, i.e., the same set of equations as we use to describe our desired shape. In this formulation, the shape is given by equations 7.1 and 7.2:

$$Y_c = g\left(\frac{1}{x_m^2}\right)\left[2x_m\frac{x}{c} - \left(\frac{x}{c}\right)^2\right], \quad x \le x_m \qquad (7.1)$$

$$Y_c = g\left(\frac{1}{1-x_m}\right)^2\left[1 - 2x_m + 2x_m\frac{x}{c} - \left(\frac{x}{c}\right)^2\right], \quad x > x_m \qquad (7.2)$$

where Y_c (the original NACA camber line) incorporates coefficients found to be effective by experimental means, x is the position along the abscissa, x_m is the position of maximum camber as a fraction of the chord, c, and g is the maximum camber. The resulting optimized thickness distributions are shown in figure 8, while the deflected shapes are depicted in figure 9.

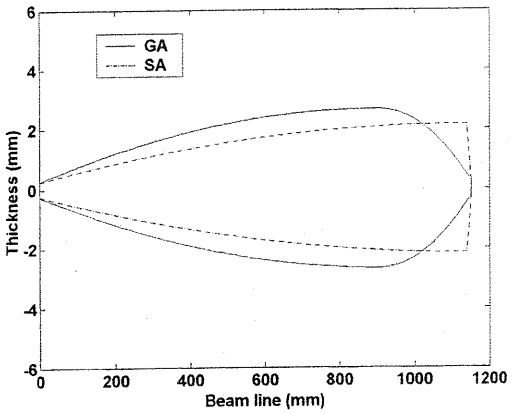

Figure 8: Optimal thickness distributions with polynomial parameterization.

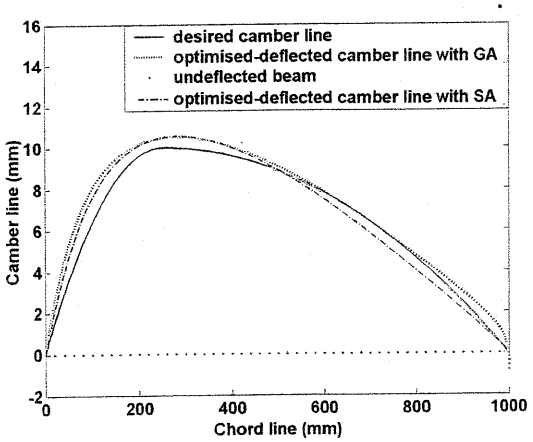

Figure 9: Optimized camber lines obtained with the polynomial parameterization using GA (min error=25.71 mm^2) and SA (min error=26.85 mm^2).

A wing geometry, and in particular the camber line, can also be defined by *spline curves* (B-splines, Hermite functions, Bézier curves, NURBS[19,20,21]). Bézier forms are a special case of B-spline curves. Cubic B-splines curves are numerically more stable than curves in the piecewise cubic Hermite form. B-splines form a basis for all splines, so any spline curve can be written as a B-spline. We have used NURBS (Non-Uniform Rational B-Splines), considering as design variables the position of the control points of these curves.

The basic formulation of NURBS is given by a set of equations 8.1, 8.2 and 8.3, as follows:

$$P(u) = \sum_{i=0}^{n} R_{i,p}(u) P_i \tag{8.1}$$

$$R_{i,p}(u) = \frac{N_{i,p}(u) w_i}{\sum_{j=0}^{n} N_{j,p}(u) w_i} \tag{8.2}$$

$$N_{i,0} = \begin{cases} 1, & if \quad u_i \le u < u_{i+1} \\ 0, & otherwise \end{cases} \tag{8.3}$$

in which:

- $p, p_1, \ldots, p_n$ are the control points, each of which is associated with a non-negative weight w_i;
- the knot vector $U=\{u_0, u_1, \ldots u_m\}$ of $m+1$ knots;
- $N_{i,p}$ are the NURBS basis functions of degree p;
- the number of knots is $m+1$, the degree of the basis functions is p, and the number of degree p basis functions is $n+1$, and $m=n+p+1$;
- local support is a non-zero on $[u_i, u_{i+p+1})$ and
- the basis function $R_{i,p}(u)$ is a composite curve of degree p rational functions with joining points at knots in $[u_i, u_{i+p+1}]$.

To create the design curves or surfaces, here we have used Dassault Systemes' CATIA V5 CAD system. The NURBS curve is the fundamental data structure of a V5 curve. The geometry of the beam is here modeled using unit control point weights, with control point locations forming the design variables. Figure 10 shows the thickness distribution along the beam after the optimization process. The optimized deflected camber can be seen in figure 11.

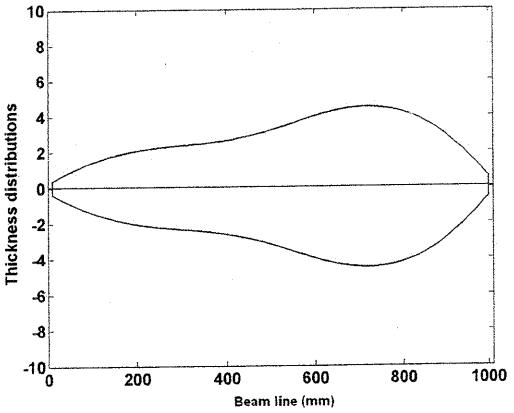

Figure 10: Optimal thickness distribution with NURBS approach.

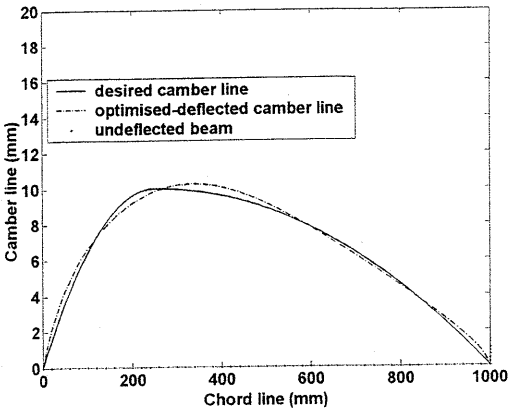

Figure 11: Optimized camber line obtained with the NURBS parameterization using GA (min error=9.10 mm^2).

To summarize, we have used Discrete, Hicks-Henne, Polynomial and NURBS geometry parameterizations and searched using local Simulated Annealing and Genetic Algorithm methods to design a beam structure that deforms to give airfoil shapes in the post-buckled regime, see table 1. As depicted in figures 4, 6, 8 and 10, the thickness of the beam tends to increase gradually at the RH end, as the beam needs to be stiffer there, while in the region of maximum camber, it is less stiff, in order to match the curvature of the desired deflection, not unlike the battens used in racing sails. Figures 6 and 8 show no inflection of the thickness (i.e., the distribution is quasi-linear) but the resulting accuracy is then poor. As a result of this study we choose to use the GA / NURBS approach in further work as it gives good results and smooth geometries.

Parameterization	Errors (mm^2)	
	Using GA	Using SA
Discrete	7.23	9.54
Hicks-Henne	11.07	31.97
Polynomial	25.71	26.85
NURBS	9.10	

Table 1: Summary of beam optimizations

We next turn to the use of these results as the starting points for the plate designs that would be used to support full wing geometries.

PLATES

In real aircraft operations we desire the shape of the whole wing to alter from one configuration to another by the application of simple forces. So far we have concentrated on achieving a single known camber shape. Next we seek plate geometries that can move from one deflected shape to another by simply

varying applied end loads. This requires suitable surface parameterizations and we can use essentially the same techniques as already described. We commence by taking solutions obtained for the 2D strut models and extruding them into 3D.

If we take the geometry of figure 10 and create a wing plate that is 1600mm wide and 1000mm deep and then load it eccentrically and non-uniformly along its edge we gain control of the whole wing, see figure 12.

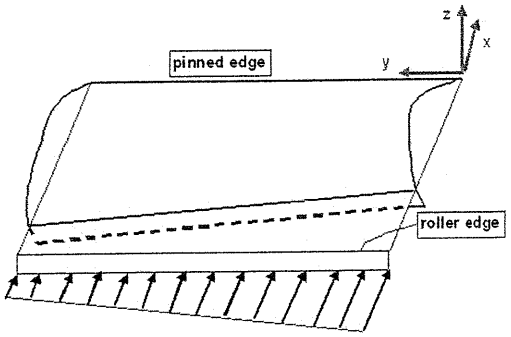

Figure 12: The lateral deflected shape of a plate, under a compressive non-uniform distributed load

To begin we will consider two cases: one with only two point loads, one at each corner and one with a linearly varying load. The point loads model would, of course, be easier to control in terms of using actuators to achieve the required shapes. In both cases the loading is defined by the value at the two extreme edges and so it is possible to produce contour maps of deflection as these two quantities change. These are plotted in figures 13, 14, 15 and 16. In both cases some of the calculations become unstable and so the plots show regions where there is a lack of continuity as the forces alter. Nonetheless the overall trends can clearly be seen. These show that a range of camber variations can be achieved with these simple forcing arrangements, although rather higher forces are needed if simple point loads are used.

The resulting deflected shapes for several particular loading cases are plotted in figures 17 and 18 and compared to equivalent NACA shapes. While the basic trends desired are apparent these are, however, not so accurate in terms of the NACA four digit family as the original strut model. To improve on the agreement with the desired NACA shapes would require further optimization effort, but now using plate analyses and also varying the plate properties both along the camber-line and across the span. Studies in this direction are ongoing at the time of writing.

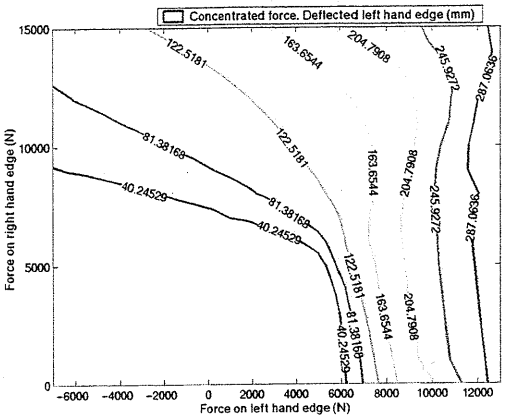

Figure 13: Contour plot of the plate response on its left-hand edge – point forcing

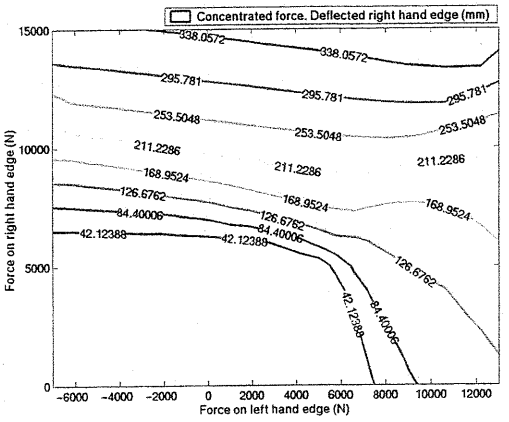

Figure 14: Contour plot of the plate response on its right-hand edge – point forcing

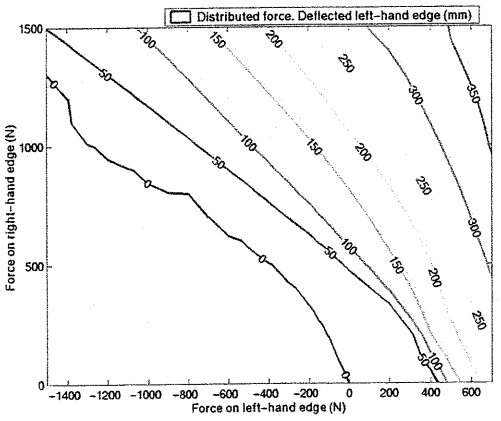

Figure 15: Contour plot of the plate response on its left-hand edge – linearly varying load

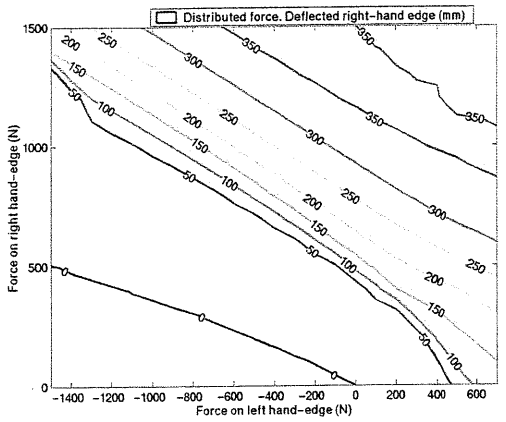

Figure 16: Contour plot of the plate response on its right-hand edge – linearly varying load

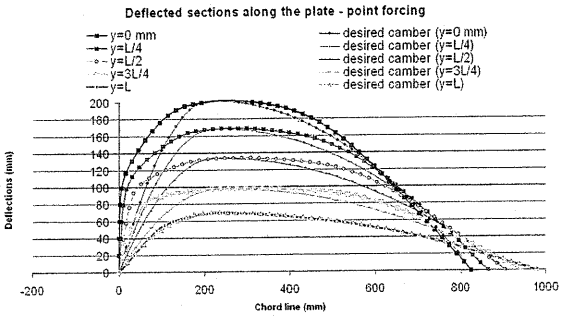

Figure 17: Deflected shapes of four equally spaced sections along the plate – point forcing

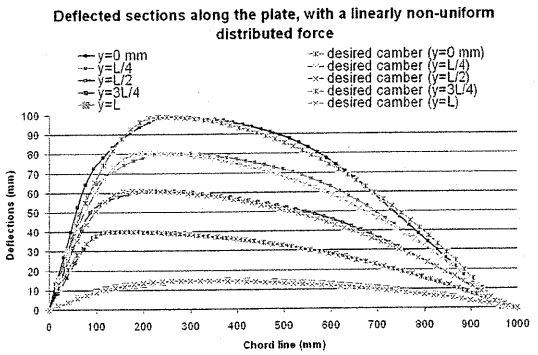

Figure 18: Deflected shapes of four equally spaced sections along the plate – linearly varying load

CONCLUSIONS

A number of shape definition schemes have been assessed for use in providing a deformable airfoil spinal structure. These include direct control of the properties of the finite element mesh, polynomial models, Hicks-Henne functions and the NURBS capabilities of the CATIA V5 CAD system. We have used these parameterizations to carry out inverse design work on strut models using two global optimizers (a genetic algorithm and simulated annealing). To date we have found that good approximations to the camber lines found in NACA four digit airfoils may be readily achieved using 0.3% eccentric end loads, genetic algorithm searches and either direct control of the meshes or via the CAD code (the latter obviously has advantages when considering plate models). Overall, the GA applied to a discrete 14 variable model gives the most accurate control of deflected shape, although the resulting geometry is not smooth. Of the smooth shape control parameterizations studied here, the NURBS method gives best control, and is only slightly less accurate than the discrete method.

We have also carried out preliminary studies of plate deflections models and shown that varying camber control can be achieved over wing-like structures using just two localized forces. To date these have been directly based on the optimization of two dimensional strut models which have then been extruded to create full plate systems. Future work will address searches across fully three dimensional structures.

REFERENCES

[1] Stanewsky, E., *Adaptive wing and flow control technology*, Prog. Aero. Sci., 37, 583-667, 2001.

[2] Sanders B., Eastep F. E. and Forster E., *Aerodynamic and aeroelastic characteristics of wings with conformal control surfaces for morphing aircraft*, J. Aircraft, Vol. 40, No. 1, 94-99, 2003.

[3] Autsin, F., Rossi, M. J., Van Nostrand, W., Knowles, G. and Jameson, A., *Static shape control for adaptive wings*, AIAA J., Vol. 32, No. 9, 1895 -1901, 1994.

[4] McGuire, Willian, Gallagher, Richard H., Ziemian, Ronald, *Matrix Structural Analysis*, 2000

[5] Reddy, J. N., *Finite Element Method*, 143-208, 594 -598, 1993.

[6] Cook,Robert D., David S. Malkus, Michael E. Plesha, Concepts and applications of finite element analysis, 1989.

[7] Abaqus - Theory manual, 2000.

[8] Pai, P. Frank, Anderson, J. Tony, Wheater, Eric A., *Lagrange-deformation tests and total-Lagrangian finite-element analyses of flexible beam*, 1999

[9] Bažant, Zdeněk P., Cedolin, Luigi, *Stability of Structures*, 3-46, 2003.

[10] Keane, A. J., *The Options design exploration system*, 2002.

[11] Abbott, I. A., and Von Doenhoff, A. E., *Theory of Wing Sections*, Dover, New York, 1959

[12] Metropolis, N., A. Rosenbluth, A. Teller, E. Teller, *Equation of State Calculations by fast Computing Machines*, J. Chem. Phys., Vol. 21, No. 6, 1087-1092, 1953.

[13] Samareh, Jamshid A., *Survey of Shape parameterization Techniques for High-Fidelity Multidisciplinary Shape Optimization*, AIAA Journal, Vol.39, No.5, May 2001.
[14] Sobester, Andras, and Keane, A. J., *Empirical Comparison of Gradient-Based Methods on an Engine-Inlet Shape Optimization Problem*, AIAA/ISMO, 2002.
[15] Samareh, Jamshid A., *Novel Mutidisciplinary Shape Parameterization Approach*, J. Aircraft, Vol.38, No.6, Nov-Dec 2001.
[16] Samareh, Jamshid A., *Use of CAD geometry in MDO*, 6th AIAA/ISSMO September 4-6, 1996.
[17] Hicks, R., Henne, P., *Wing Design By Numerical Optimization*, J. Aircraft, Vol.15, No.7, 407 – 412, 1978.
[18] Reuther, James J., Jameson, Anthony, Alonso, Juan J., Rimlinger, Mark J. and Saunders, David, *Constrained Multipoint Aerodynamic Shape Optimization Using an Adjoint Formuation and Parallel Computers, Part 1*, J. Aircraft, Vol.36, No.1, 51 – 60, January-February 1999.
[19] Braibant, V., and Fleury, C., *Shape Optimal Design using B-Spline Design*, Computer Methods in Applied Mechanics and Engineering, Vol.44, 247-267, 1984.
[20] Farin, G., *Curves and Surfaces for Computer Aided Design*, 1992
[21] Piegl, Les, *The NURBS Book*, 1997.